Supporting Information

Investigating hierarchical gas confinement in high-rank coal through small-angle neutron scattering

Rui Zhang and Shimin Liu*

Department of Energy and Mineral Engineering, G^3 Center and Energy Institute, Pennsylvania State University, University Park, PA 16802, USA

Corresponding author:
*Tel. No.: +1 8148634491; Fax No.: +1 8148653248; Email: szl3@psu.edu

Figures

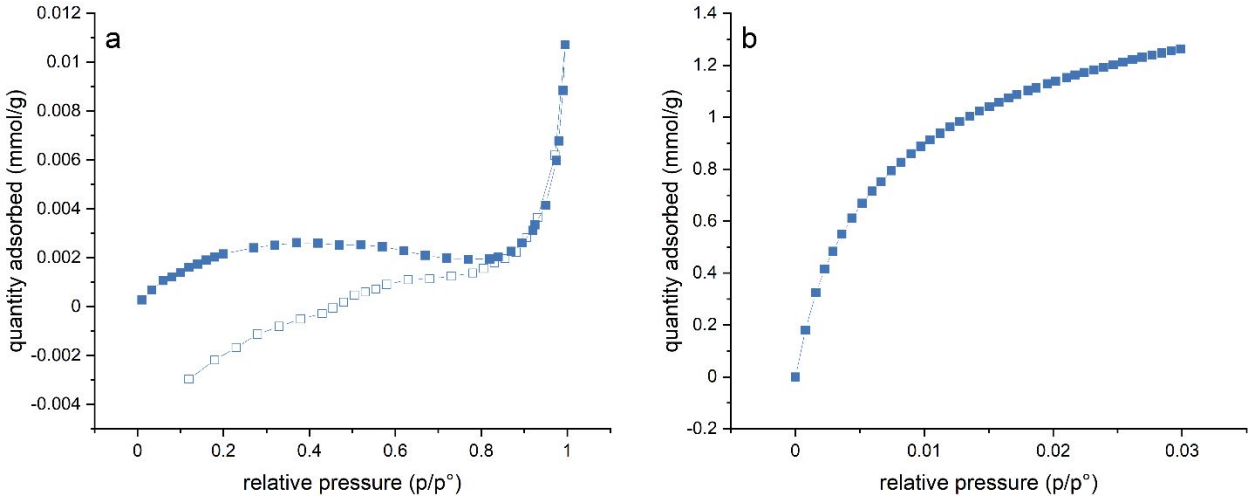

Fig. S1 Low-pressure adsorption isotherms of the Hazleton coal: (a) N_2 sorption and (b) CO_2 sorption.

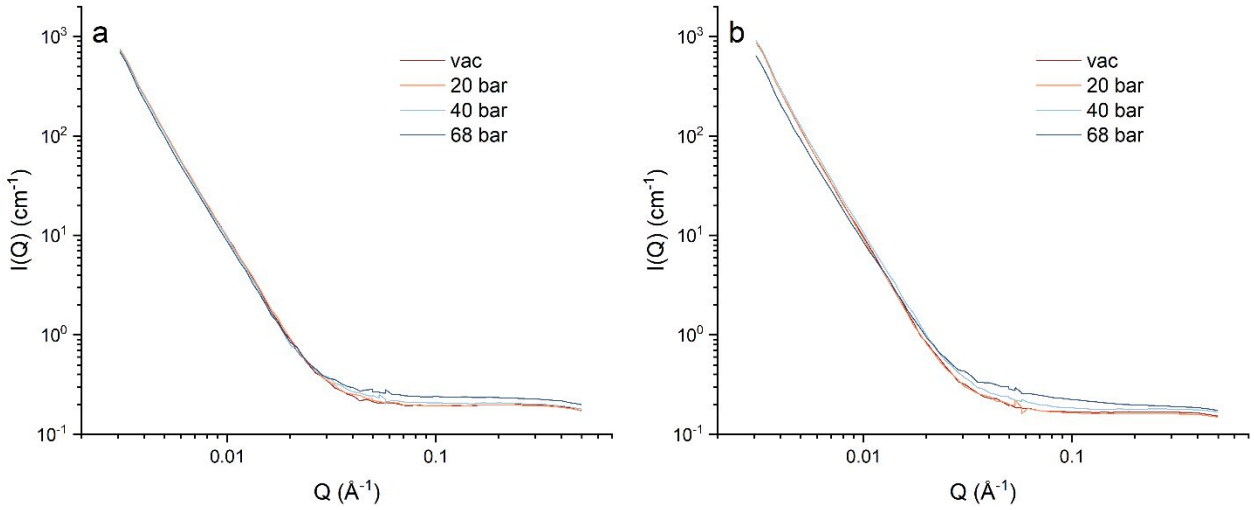

Fig. S2 Scattering intensities under (a) CD_4 and (b) CO_2 injection for the Hazleton coal powder sample.

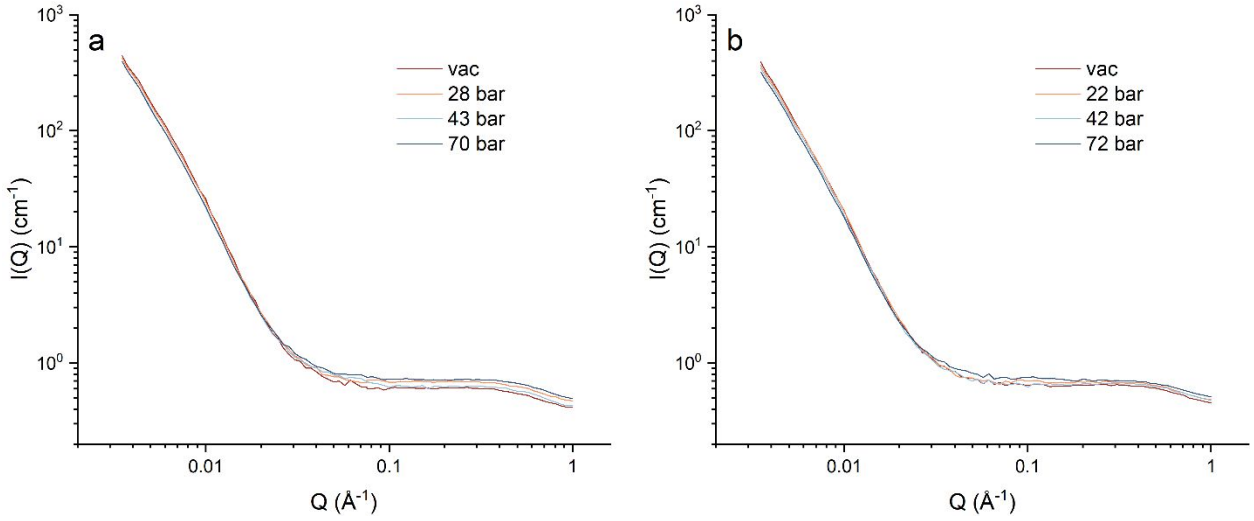

Fig. S3 Scattering intensities under (a) CD_4 and (b) CO_2 injection for the Hazleton coal thin section cut parallel to the bedding.

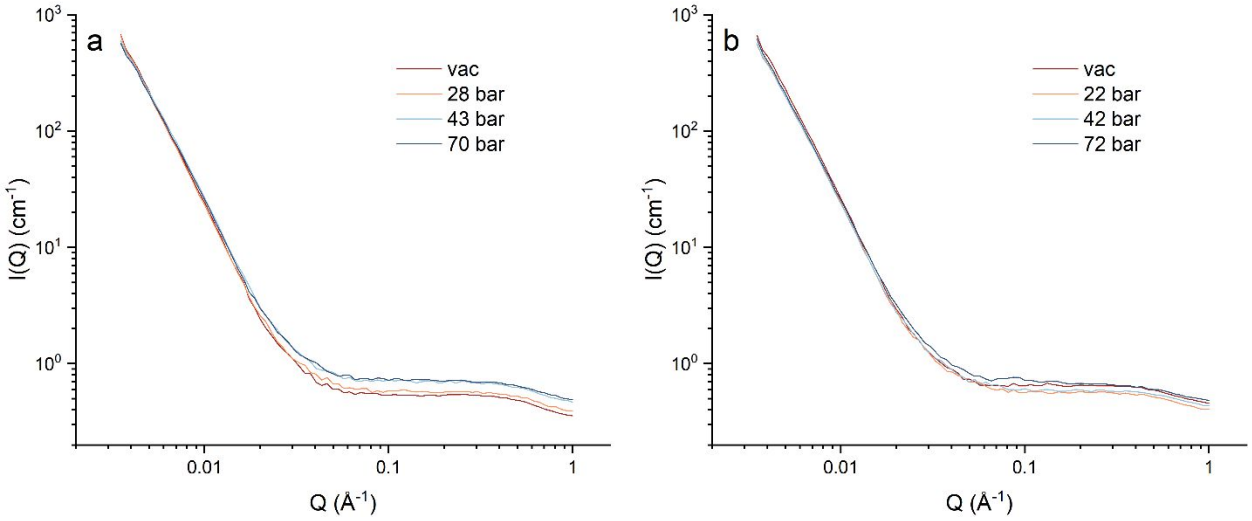

Fig. S4 Scattering intensities under (a) CD_4 and (b) CO_2 injection for the Hazleton coal thin section cut perpendicular to the bedding.

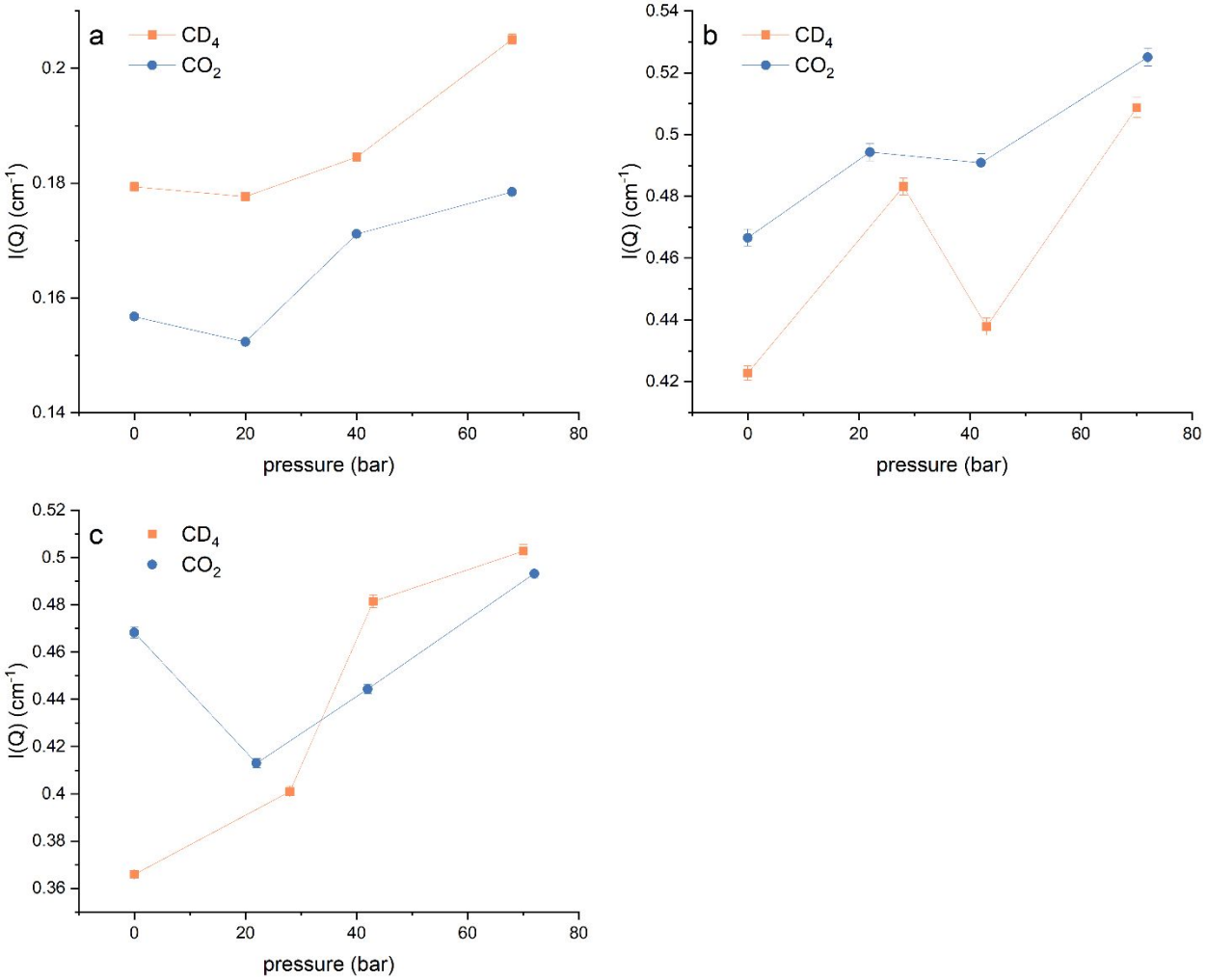

Fig. S5 Scattering backgrounds based on the slope of $I(Q)Q^4$ versus Q^4 assuming Porod law at high Q for the (a) Hazleton coal powder sample and thin section samples cut (b) parallel and (c) perpendicular to the bedding.

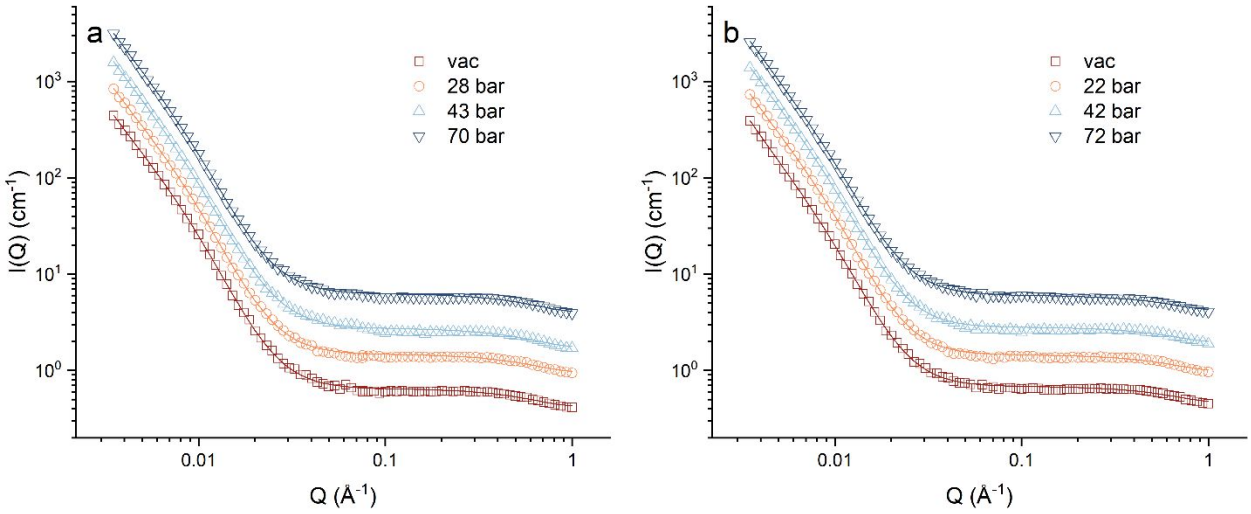

Fig. S6 Scattering intensities under (a) CD_4 and (b) CO_2 injection for the Hazleton coal thin section cut parallel to the bedding (Hollow dots are experimental data and solid lines are data-fitted results. Scattering intensities under gas injection are offset for a clear view).

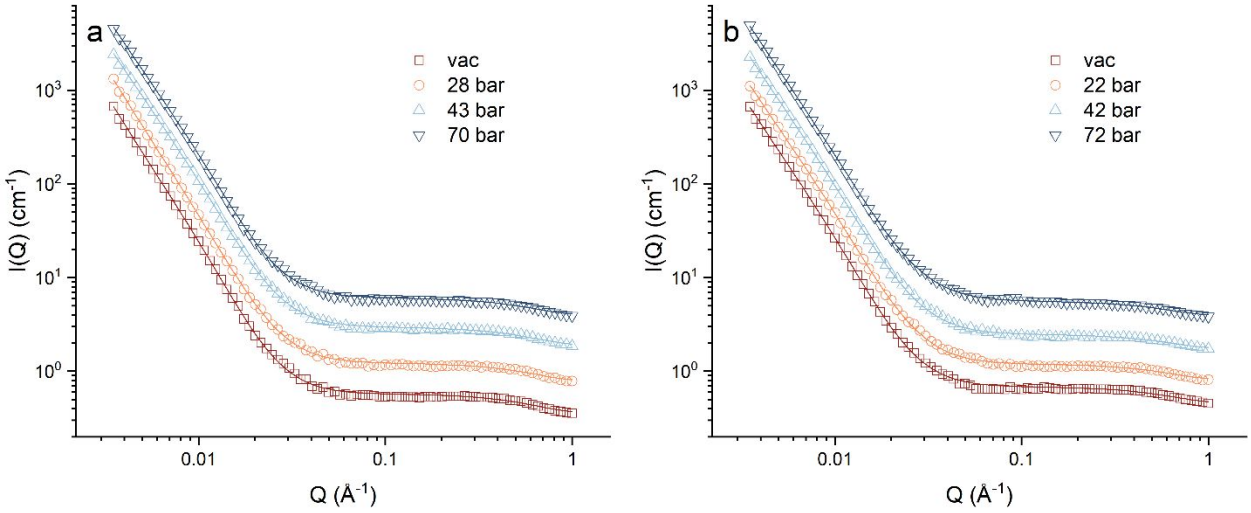

Fig. S7 Scattering intensities under (a) CD_4 and (b) CO_2 injection for the Hazleton coal thin section cut perpendicular to the bedding (Hollow dots are experimental data and solid lines are data-fitted results. Scattering intensities under gas injection are offset for a clear view).

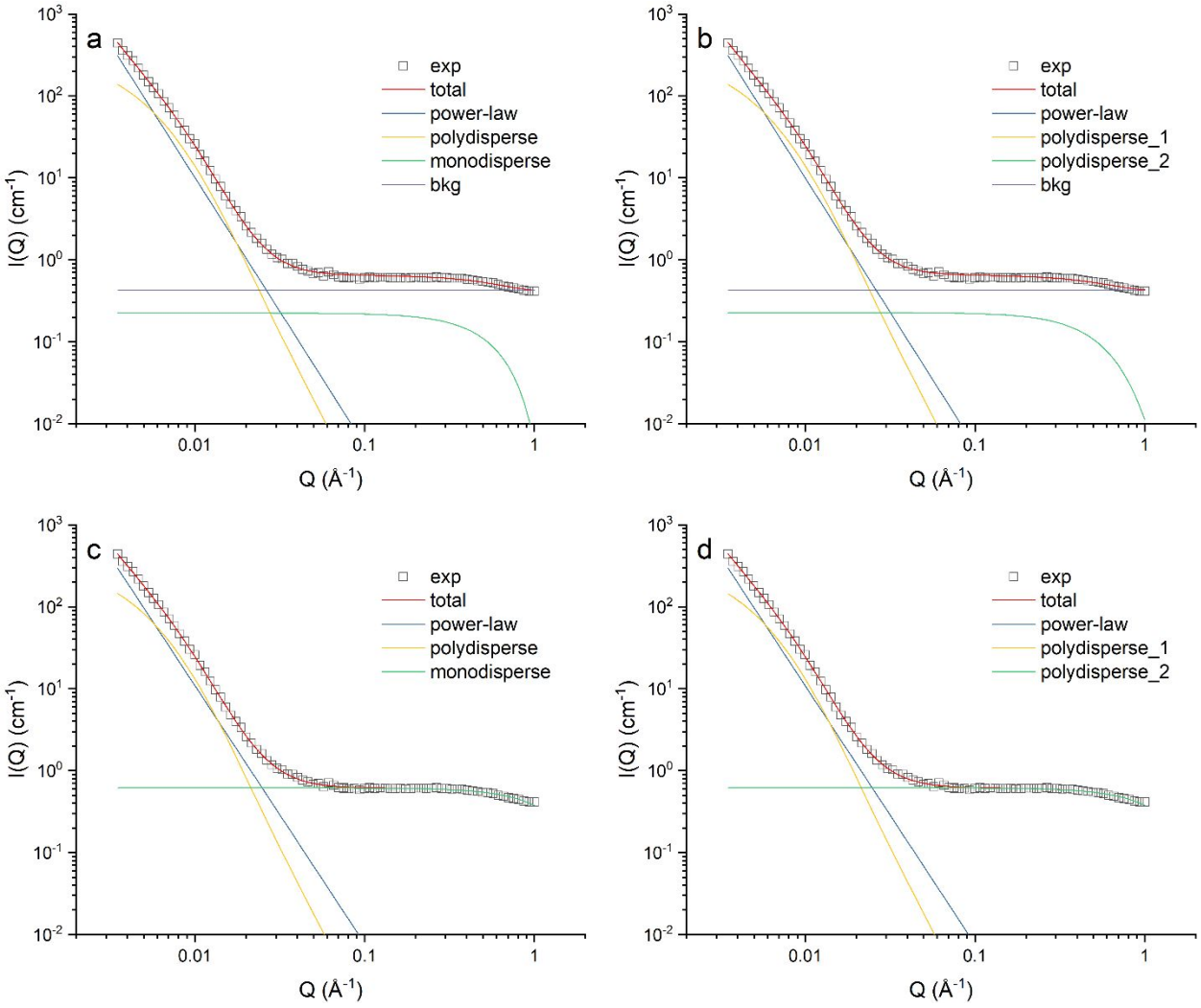

Fig. S8 Different data-fitting strategies on the scattering intensity under vacuum for the Hazleton coal thin section cut parallel to the bedding (Hollow dots are experimental data and solid lines are data-fitted results).

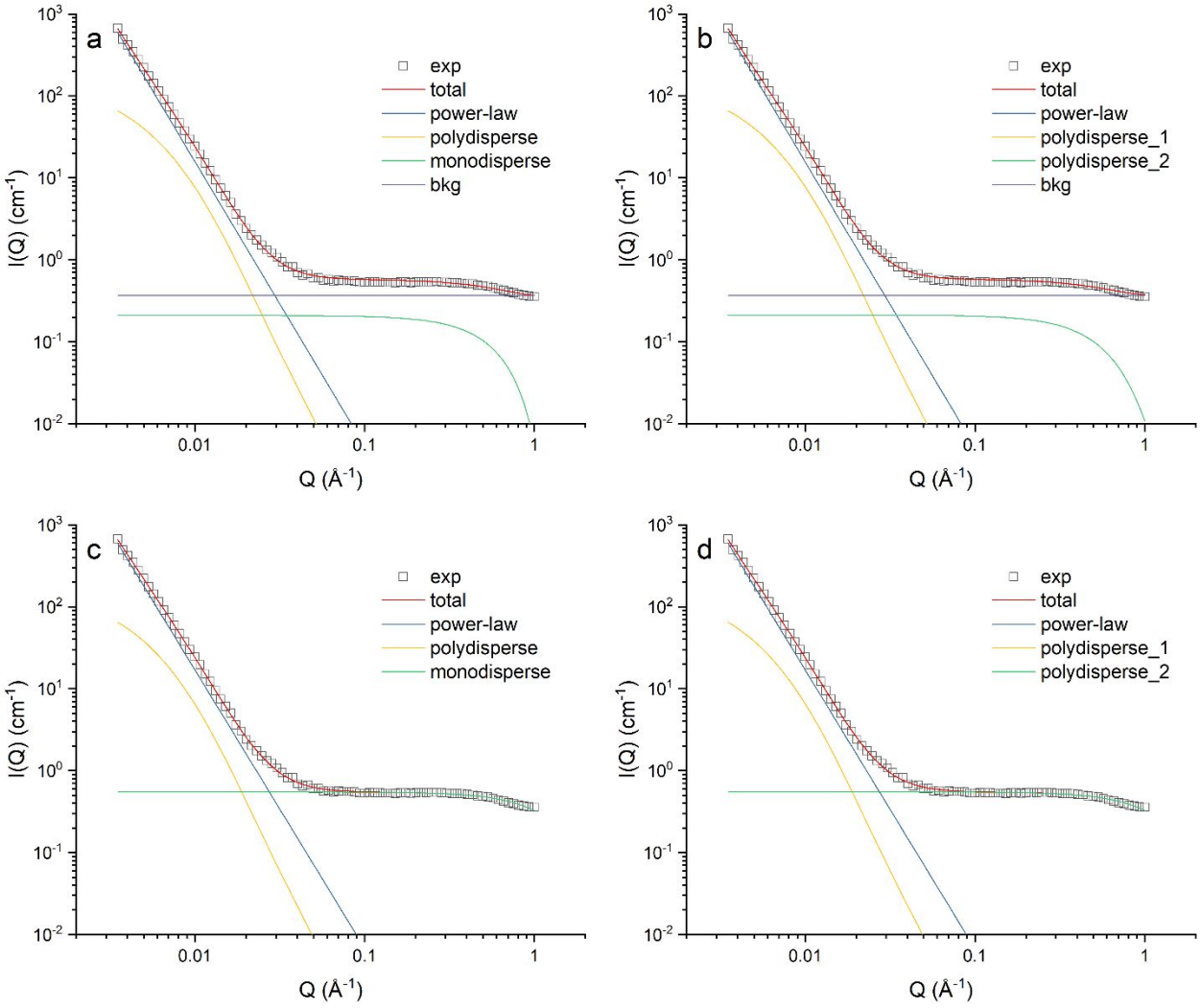

Fig. S9 Different data-fitting strategies on the scattering intensity under vacuum for the Hazleton coal thin section cut perpendicular to the bedding (Hollow dots are experimental data, and solid lines are data-fitted results).

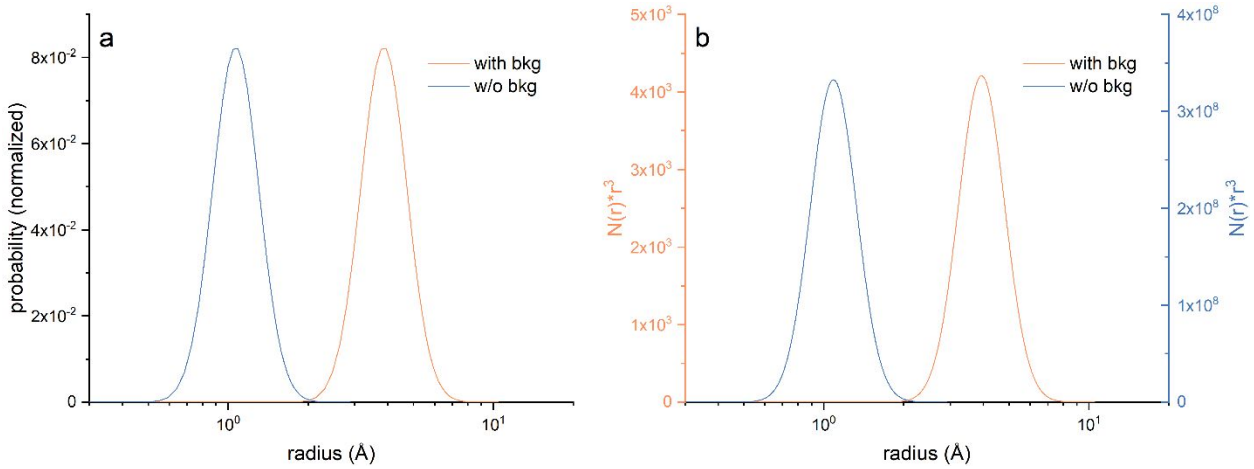

Fig. S10 Probability density functions of micropores based on the fitting of the scattering intensity under vacuum with and without considering scattering background for the Hazleton coal powder sample: (a) sasview package; (b) sasfit package.

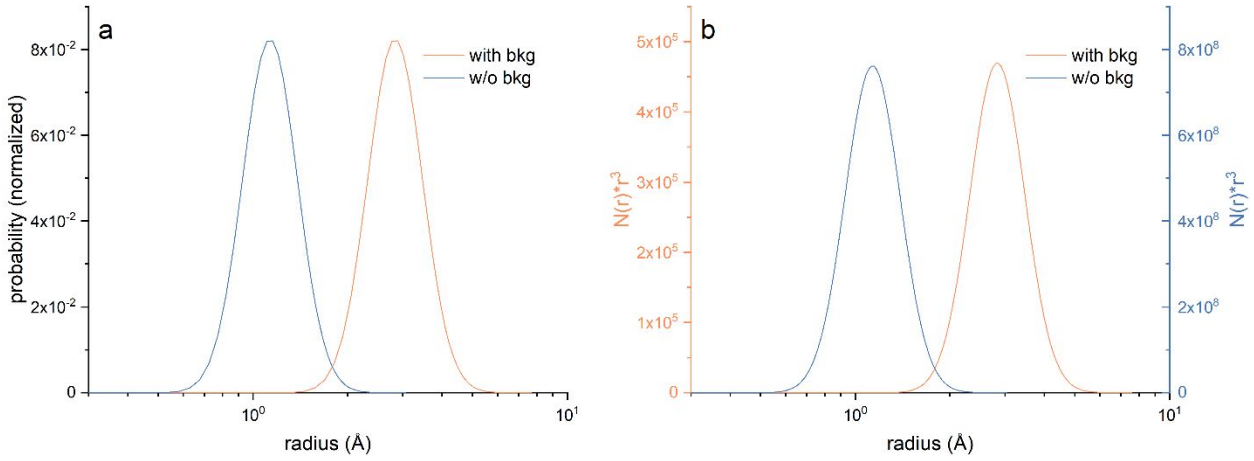

Fig. S11 Probability density functions of micropores based on the fitting of the scattering intensity under vacuum with and without considering scattering background for the Hazleton coal thin section cut parallel to the bedding: (a) sasview package; (b) sasfit package.

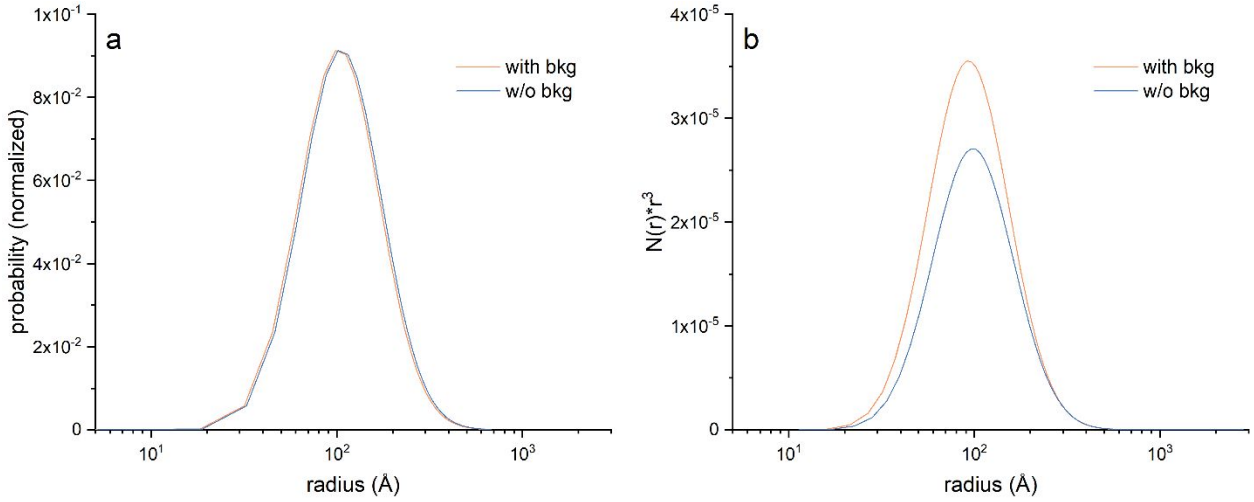

Fig. S12 Probability density functions of mesopores based on the fitting of the scattering intensity under vacuum with and without considering scattering background for the Hazleton coal thin section cut parallel to the bedding: (a) sasview package; (b) sasfit package.

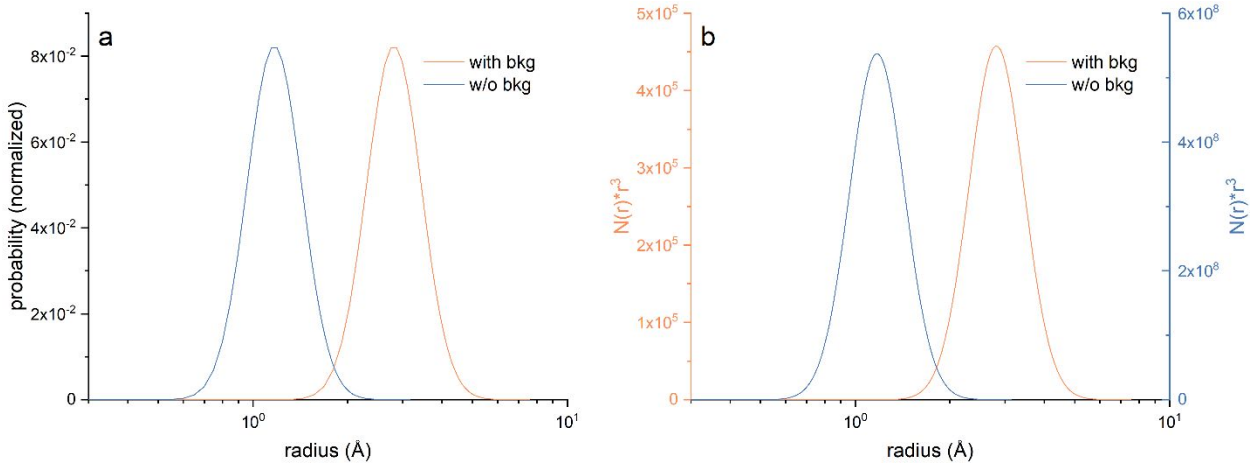

Fig. S13 Probability density functions of micropores based on the fitting of the scattering intensity under vacuum with and without considering scattering background for the Hazleton coal thin section cut perpendicular to the bedding: (a) sasview package; (b) sasfit package.

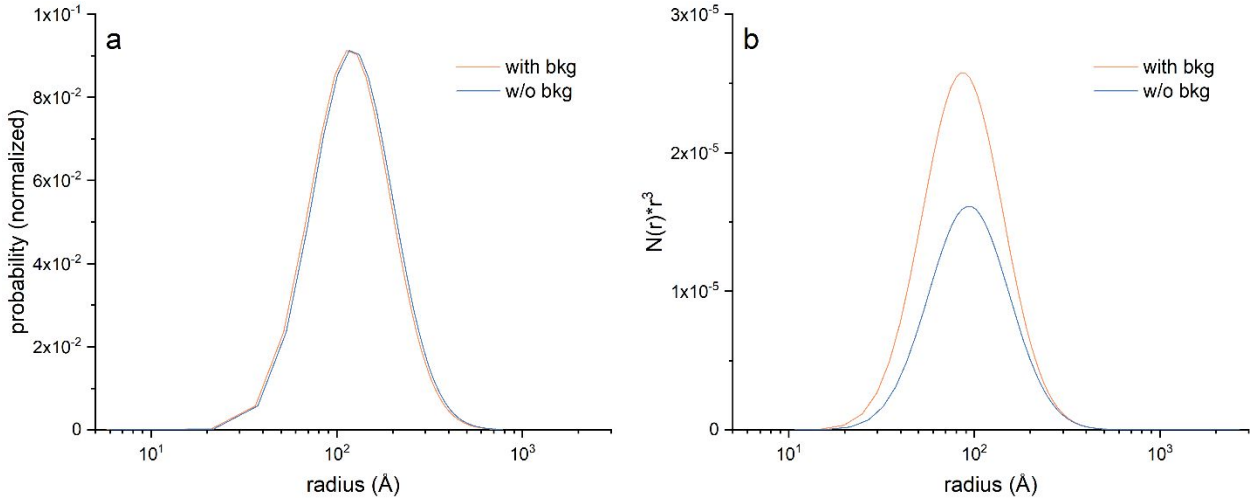

Fig. S14 Probability density functions of mesopores based on the fitting of the scattering intensity under vacuum with and without considering scattering background for the Hazleton coal thin section cut perpendicular to the bedding: (a) sasview package; (b) sasfit package.

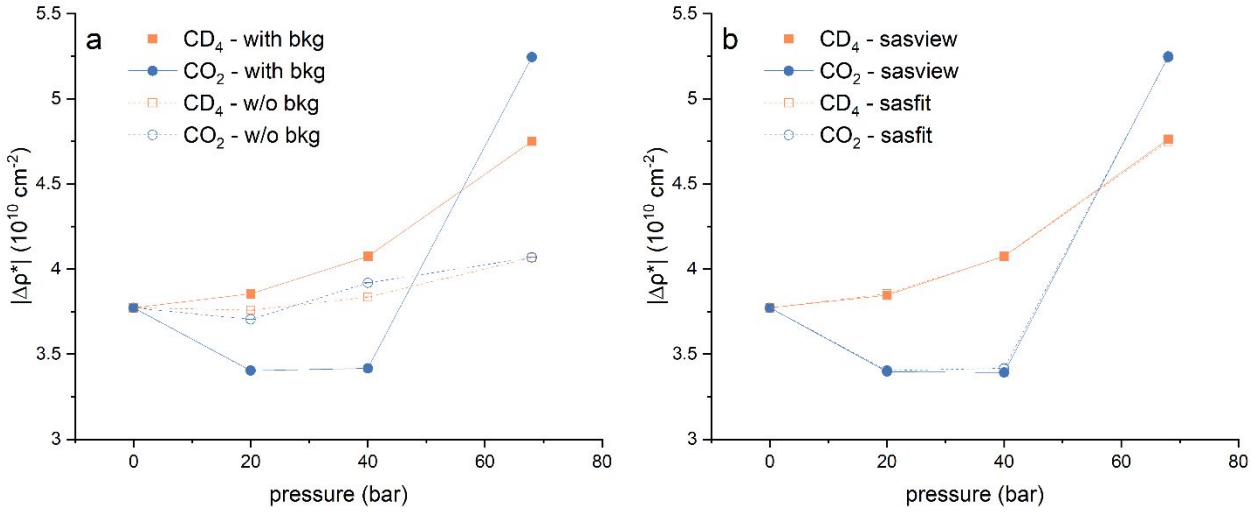

Fig. S15 Scattering contrast as a function of pressure in micropores for the Hazleton coal powder sample.

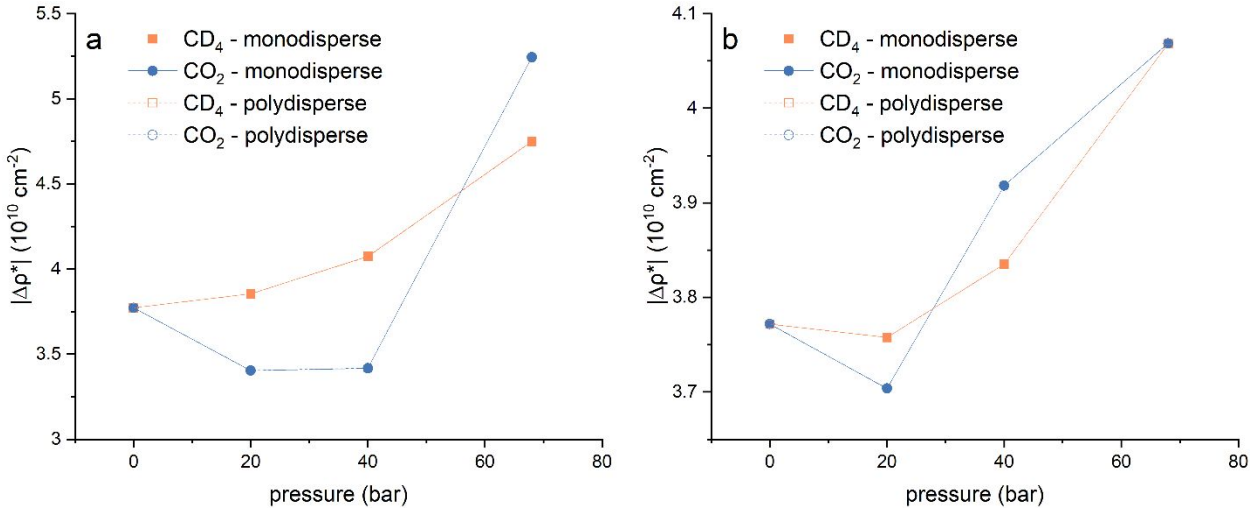

Fig. S16 Scattering contrast as a function of pressure in micropores for the Hazleton coal powder sample.

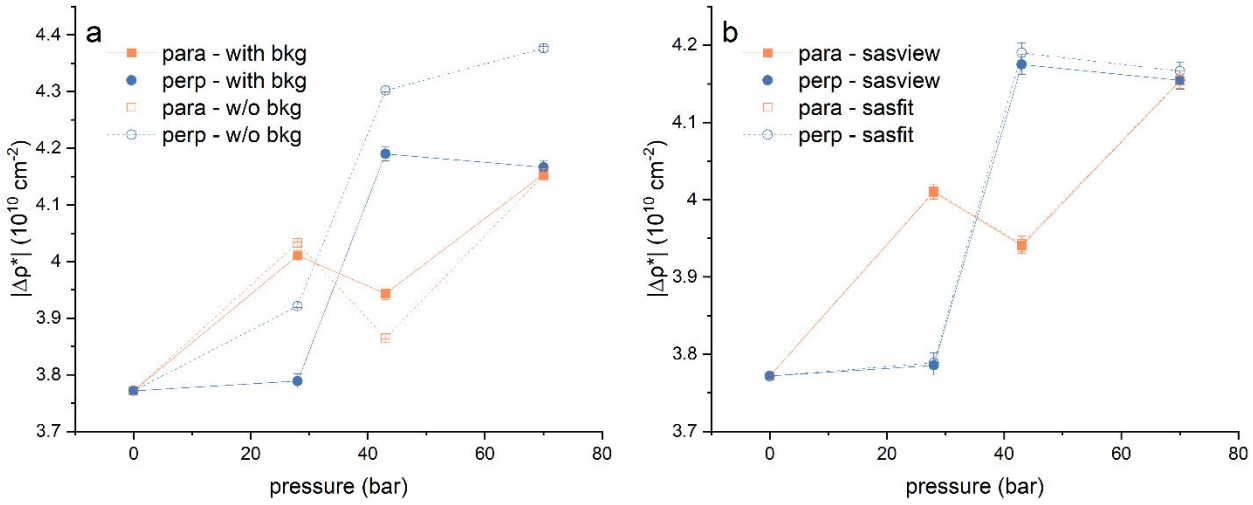

Fig. S17 Scattering contrast as a function of pressure in micropores during CD_4 injection for the Hazleton coal thin section samples.

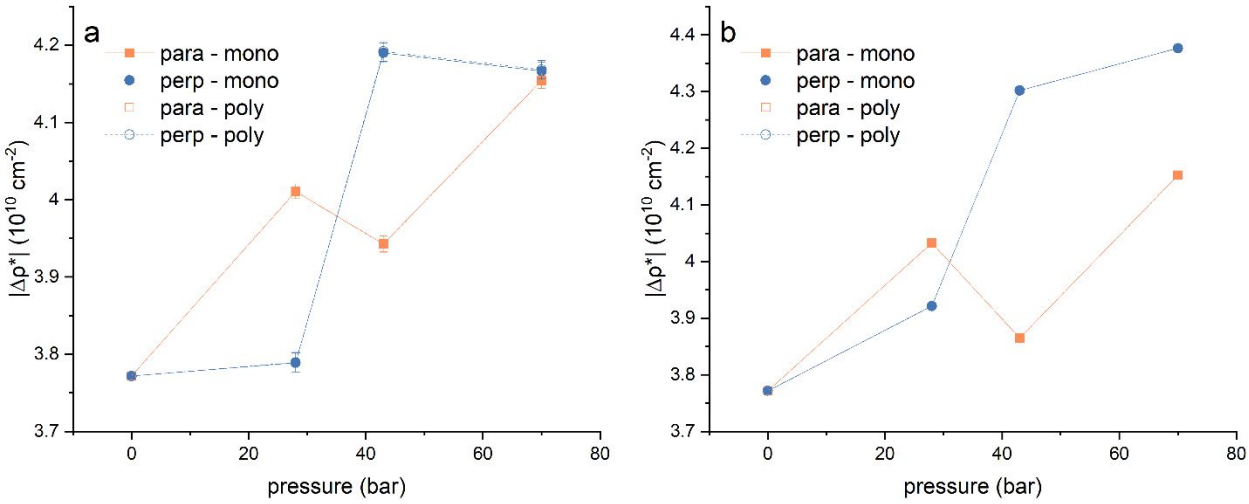

Fig. S18 Scattering contrast as a function of pressure in micropores during CD_4 injection for the Hazleton coal thin section samples: (a) consider background; (b) without consider background.

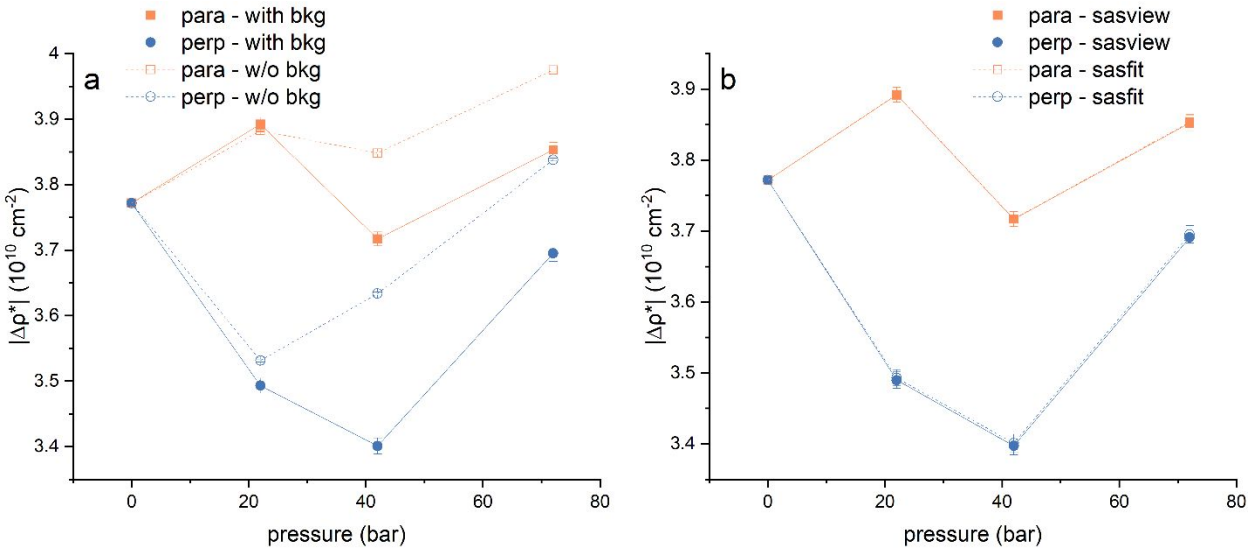

Fig. S19 Scattering contrast as a function of pressure in micropores during CO_2 injection for the Hazleton coal thin section samples.

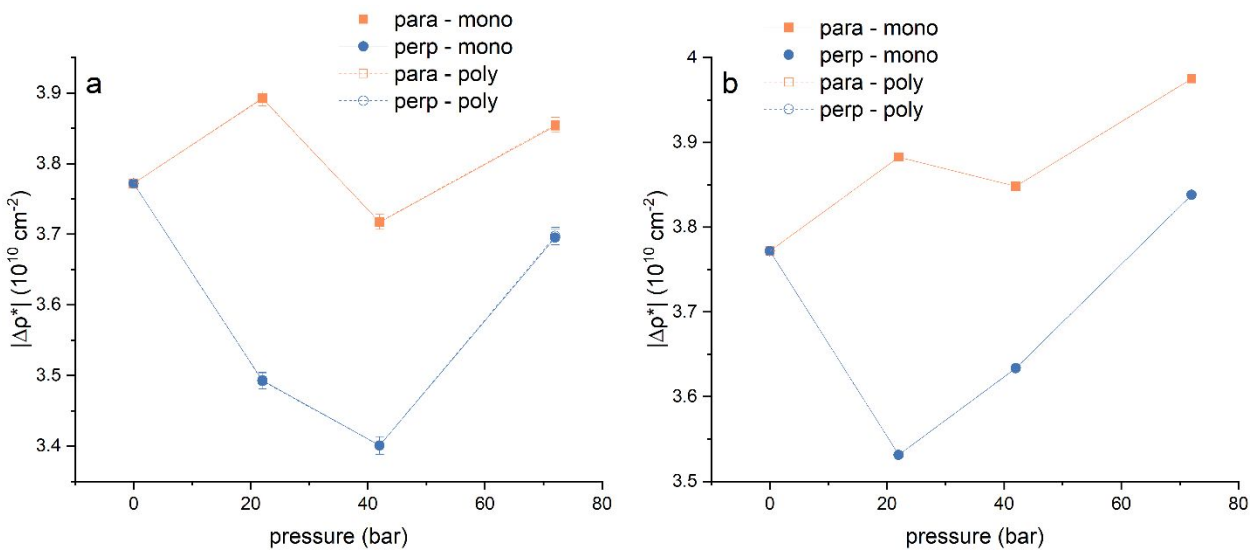

Fig. S20 Scattering contrast as a function of pressure in micropores during CO_2 injection for the Hazleton coal thin section samples: (a) consider background; (b) without consider background.

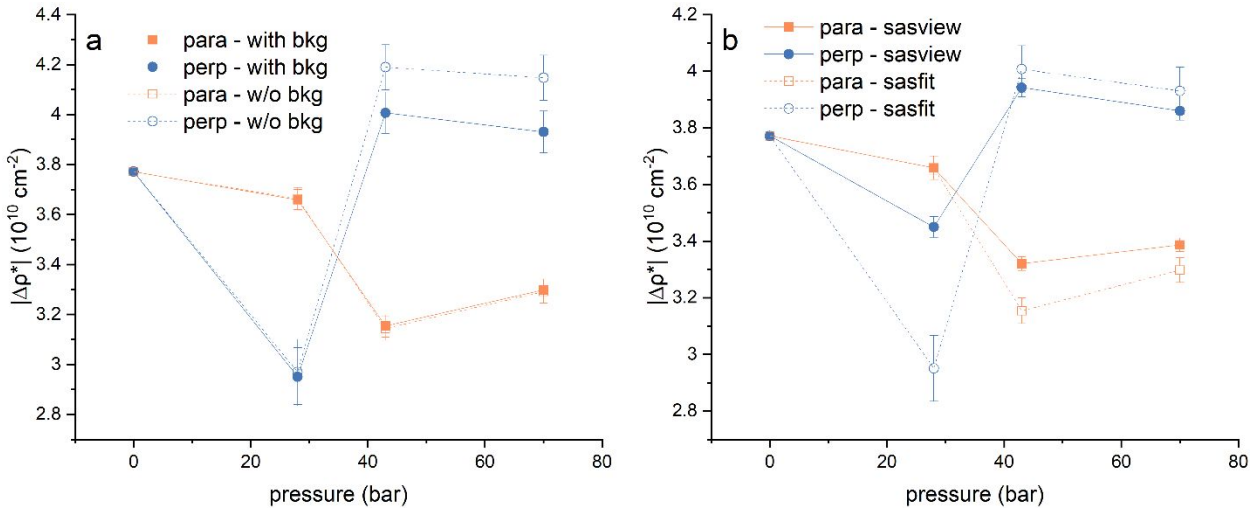

Fig. S21 Scattering contrast as a function of pressure in mesopores during CD_4 injection for the Hazleton coal thin section samples.

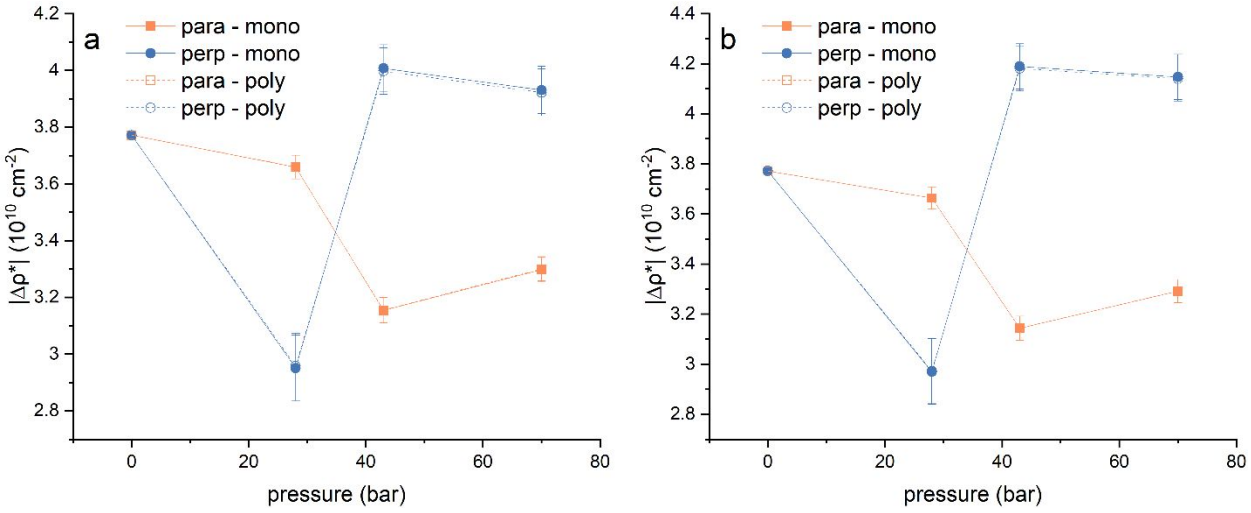

Fig. S22 Scattering contrast as a function of pressure in mesopores during CD_4 injection for the Hazleton coal thin section samples: (a) consider background; (b) without consider background.

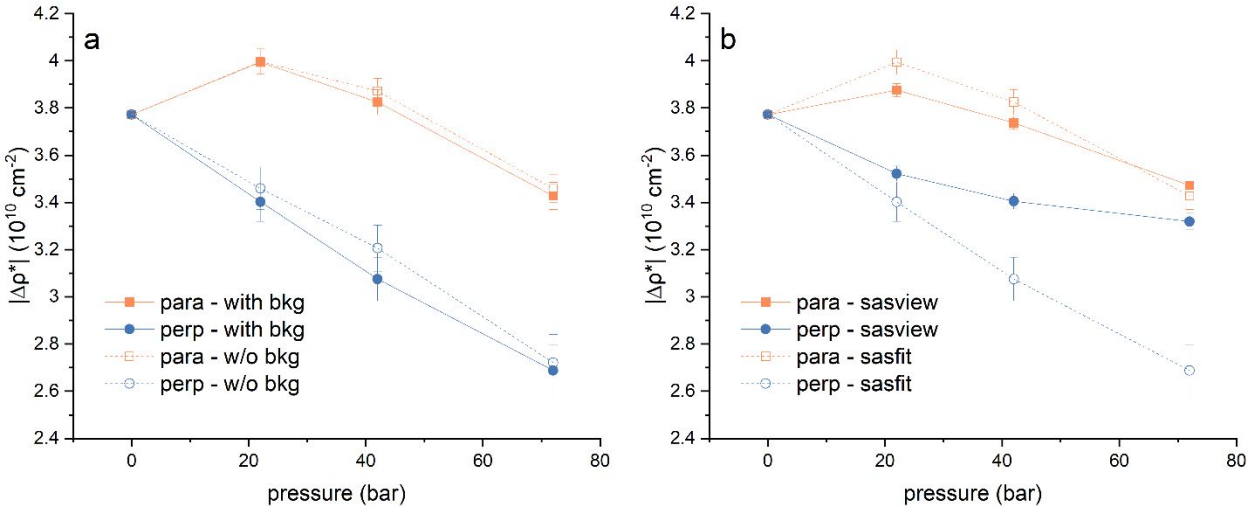

Fig. S23 Scattering contrast as a function of pressure in mesopores during CO_2 injection for the Hazleton coal thin section samples.

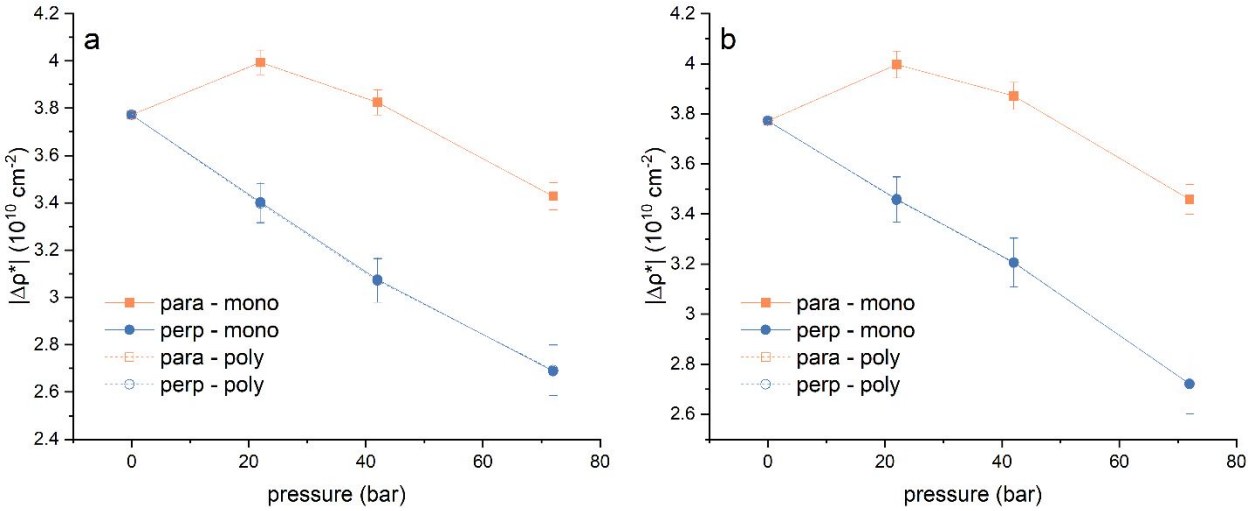

Fig. S24 Scattering contrast as a function of pressure in mesopores during CO_2 injection for the Hazleton coal thin section samples: (a) consider background; (b) without consider background.

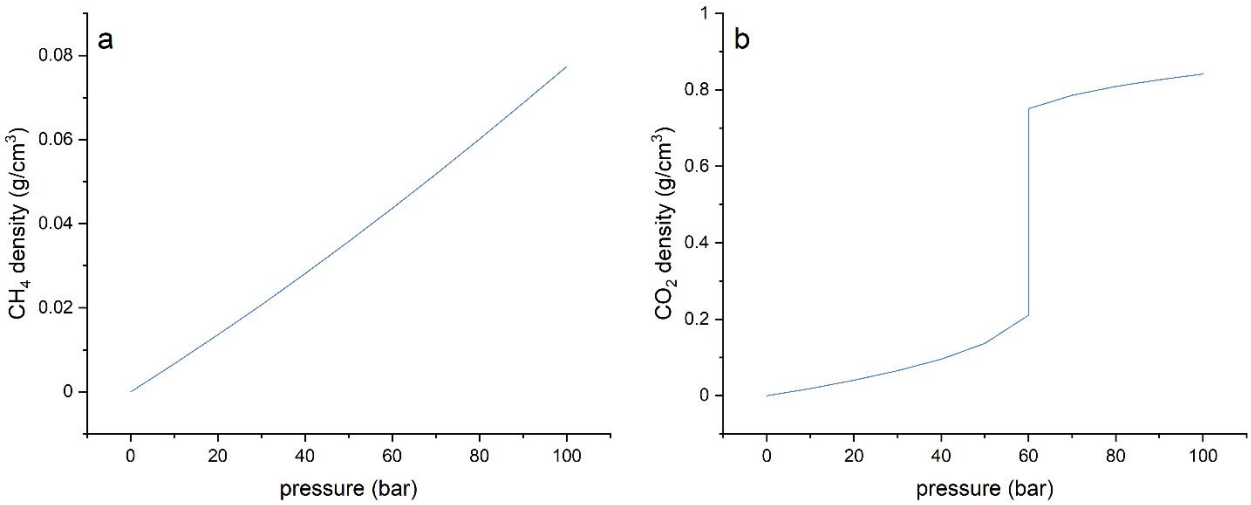

Fig. S25 Bulk densities of (a) CH_4 and (b) CO_2 under room temperature.

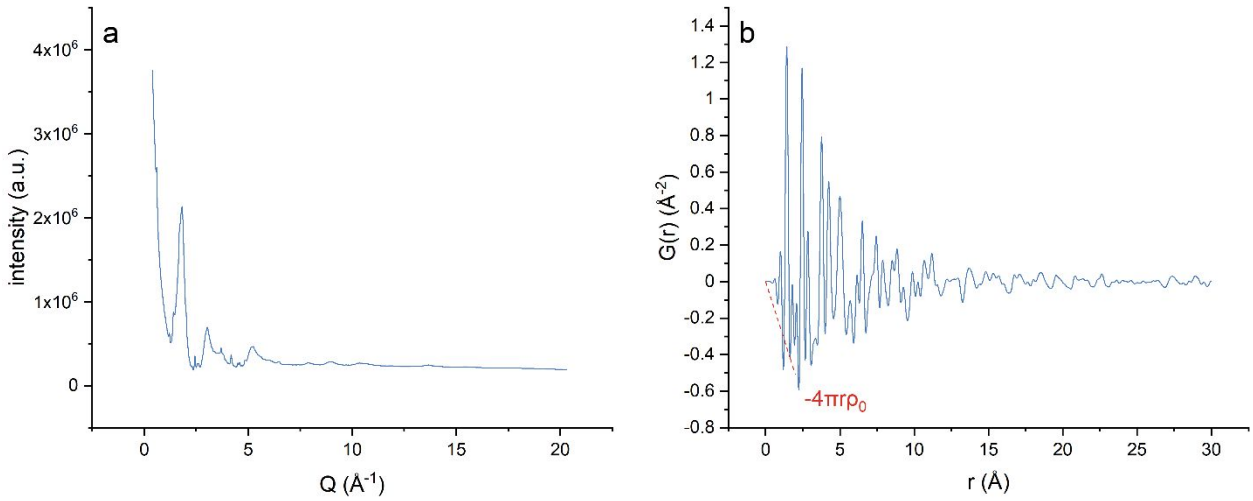

Fig. S26 (a) The measured total scattering intensity without absolute intensity calibration and (b) the estimated atomic pair distribution function of the Hazleton coal.

Tables

Table S1 Ultimate analysis of the Hazelton coal

Volatile	5.70 wt%
Fixed carbon	82.14 wt%
Ash	12.16 wt%
Sulfur	1.60 wt%
Carbon	81.06 wt%
Hydrogen	1.81 wt%
Nitrogen	0.90 wt%
Oxygen	2.47 wt%

Table S2 Data-fitting assuming monodisperse sphere in micropores for the Hazleton powder sample

Package	Treatment	Micropore radius (Å)
sasfit	with bkg	5.294±0.058
	w/o bkg	1.494±0.012
sasview	with bkg	5.201±0.061
	w/o bkg	1.464±0.012

Table S3 Data-fitting assuming polydisperse sphere in micropores for the Hazleton powder sample

Package	Treatment	Micropore radius (Å)
sasfit	with bkg	4.097±0.051
	w/o bkg	1.133±0.009
sasview	with bkg	4.019±0.053
	w/o bkg	1.112±0.009

Table S4 Data-fitting assuming monodisperse sphere in micropores for the Hazleton thin section sample cut parallel to the bedding

Package	Treatment	Micropore radius (Å)	Mesopore radius (Å)
sasfit	with bkg	3.681±0.018	119.844±2.317
	w/o bkg	1.536±0.006	126.424±2.557
sasview	with bkg	3.683±0.018	132.240±1.332
	w/o bkg	1.530±0.006	135.790±1.414

Table S5 Data-fitting assuming polydisperse sphere in micropores for the Hazleton thin section sample cut parallel to the bedding

Package	Treatment	Micropore radius (Å)	Mesopore radius (Å)
sasfit	with bkg	2.946±0.016	119.289±2.290
	w/o bkg	1.181±0.004	126.043±2.547
sasview	with bkg	2.949±0.016	131.980±1.324
	w/o bkg	1.179±0.004	135.590±1.410

Table S6 Data-fitting assuming monodisperse sphere in micropores for the Hazleton thin section sample cut perpendicular to the bedding

Package	Treatment	Micropore radius (Å)	Mesopore radius (Å)
sasfit	with bkg	3.660±0.020	111.755±4.272
	w/o bkg	1.586±0.007	120.506±5.712
sasview	with bkg	3.657±0.021	151.610±2.226
	w/o bkg	1.579±0.007	156.280±2.364

Table S7 Data-fitting assuming polydisperse sphere in micropores for the Hazleton thin section sample cut perpendicular to the bedding

Package	Treatment	Micropore radius (Å)	Mesopore radius (Å)
sasfit	with bkg	2.927±0.018	111.077±4.147
	w/o bkg	1.221±0.005	119.929±5.624
sasview	with bkg	2.923±0.019	151.260±2.214
	w/o bkg	1.217±0.005	155.990±2.357